AD-A246 960

REPORT DOCUMENTATION PAGE

Form Approved OMB No. 0704-0188

1a. REPORT SECURITY CLASSIFICATION: Unclassified	1b. RESTRICTIVE MARKINGS
2a. SECURITY CLASSIFICATION AUTHORITY	3. DISTRIBUTION/AVAILABILITY OF REPORT: Distribution unlimited
2b. DECLASSIFICATION/DOWNGRADING SCHEDULE	
4. PERFORMING ORGANIZATION REPORT NUMBER(S)	5. MONITORING ORGANIZATION REPORT NUMBER(S): AFOSR-TR- 92 0088
6a. NAME OF PERFORMING ORGANIZATION: Georgia Institute of Technology; 6b. OFFICE SYMBOL (If applicable)	7a. NAME OF MONITORING ORGANIZATION: AFOSR/NA
6c. ADDRESS (City, State, and ZIP Code): School of Aerospace Engineering, Georgia Institute of Technology, Atlanta, Georgia 30332	7b. ADDRESS (City, State, and ZIP Code): AFOSR/NA, Bolling AFB DC 20332-6448
8a. NAME OF FUNDING/SPONSORING ORGANIZATION: AFOSR; 8b. OFFICE SYMBOL (If applicable): N/A	9. PROCUREMENT INSTRUMENT IDENTIFICATION NUMBER: AFOSR - 90-0247, FQ8671-9001095
8c. ADDRESS (City, State, and ZIP Code): AFOSR/NA, Bolling AFB, Washington, DC 20332	10. SOURCE OF FUNDING NUMBERS: PROGRAM ELEMENT NO. 61102F; PROJECT NO. 2308; TASK NO. A1; WORK UNIT ACCESSION NO.

11. TITLE (include Security Classification)
"Fractal Image Compression of Rayleigh, Raman, LIF and LDV Data in Turbulent Reacting Flows" (U)

12. PERSONAL AUTHOR(S)
Warren C. Strahle and Jechial I. Jagoda

13a. TYPE OF REPORT	13b. TIME COVERED	14. DATE OF REPORT (Year, Month, Day)	15. PAGE COUNT
Final	FROM 900930 TO 910929	November, 1991	6

16. SUPPLEMENTARY NOTATION

17. COSATI CODES			18. SUBJECT TERMS (Continue on reverse if necessary and identify by block number)
FIELD	GROUP	SUB-GROUP	Fractals, Turbulence, Combustion, Ramjet, Optics, Fluid Mechanics.

19. ABSTRACT (Continue on reverse if necessary and identify by block number)

Experiments and analysis were completed concerning a diagnostic program on a two dimensional subsonic windtunnel with a backward facing step and combustion. Combustibles were introduced as a hydrogen-argon mixture from a porous floor behind the step. Completed were LDV and Raman spectroscopy for mean and rms velocity (two components) and temperature. Analysis used a two equation tubulence model which predicted the gross features of the flow but somewhat underpredicted reattachment length. Two dimensional and three dimensional fractal interpolation techniques were developed for reduction of noise to signal ratio in the complex turbulent flow. New methods of fractal analysis of time series were developed.

20. DISTRIBUTION/AVAILABILITY OF ABSTRACT: [X] UNCLASSIFIED/UNLIMITED [X] SAME AS RPT. [ ] DTIC USERS	21. ABSTRACT SECURITY CLASSIFICATION: Unclassified
22a. NAME OF RESPONSIBLE INDIVIDUAL	22b. TELEPHONE (Include Area Code) / 22c. OFFICE SYMBOL

AFOSR FINAL REPORT

FRACTAL IMAGE COMPRESSION OF RAYLEIGH, RAMAN, LIF AND LDV DATA IN TURBULENT REACTING FLOWS

Co-Principal Investigators
Warren C. Strahle
Jechiel I. Jagoda

Pepared for

AIR FORCE OFFICE OF SCIENTIFIC RESEARCH
AEROSPACE SCIENCES DIRECTORATE
BOLLING AIR FORCE BASE, DC

Contract No. AFOSR-90-0247

November, 1991

GEORGIA INSTITUTE OF TECHNOLOGY
SCHOOL OF AEROSPACE ENGINEERING
ATLANTA, GEORGIA 30332

SUMMARY

As a one year follow-on to AFOSR-88-0001, completion was sought for a program of analytical modeling, development of new fractal-based methods of data analysis and application of several experimental diagnostics to an experimental flow. The flow was in a two dimensional windtunnel with a backward facing step with provision for the injection of inerts and combustibles through a porous floor behind the step. Laser based diagnostics for velocity, species and temperature measurements included LDV and Raman spectroscopy. Fractal based methods of analysis were developed to both increase signal to noise ratio and to provide better certainty in results of joint measurements (temperature and velocity) when one of the measurements (temperature) produced uncorrelated neighboring data points. Analytical modeling techniques were refined using a two equation model of turbulence, Favre averaging being used to account for variable density effects. The combustion flows used hydrogen-argon and hydrogen-nitrogen mixtures as the fuel injectant.

Major findings were a) a significantly improved method of fractal interpolation, b) development of the hidden variable method of fractal interpolation, c) success in the analysis for predicting the elongation of the reattachment length under combustion, as opposed to its value in cold flow and d) completion of the mean and rms velocity and temperature mapping of the flow field under hot flow conditions. Major problems in laser breakdown arose late in the program, however, and joint measurements of velocity and temperature could not be completed.

RESEARCH OBJECTIVES

The primary objective was to determine the limits of scientific understanding and predictability of a particular complex turbulent reacting flow. The flow field used models that in the flame stabilization region of a solid fueled ramjet. Secondary objectives included a) the development of several laser diagnostic methods operating under particularly severe conditions of signal to noise ratio, b) creation of a data base for this flow, c) the development of fractal based methods of data analysis to aid in item a) and d) modification of the analysis to affect agreement between theory and experiment.

ACCOMPLISHMENTS

Facility

The facility was developed under two prior contracts, AFOSR-83-0356 and AFOSR-88-0001, and has been fully described under documentation of those contracts. Briefly, the combustion windtunnel is a two dimensional, backward facing step facility with the provision for injection of inerts and combustibles through a porous floor behind the step. Injectants used were mixtures of hydrogen-argon and hydrogen-nitrogen. The facility simulates the flame stabilization region of a solid fueled ramjet. For scientific purposes, however, it was used as an experimental device to investigate a highly complex, turbulent, recirculatory reacting flow with mass addition and combustion.

Experimental Effort

Following data acquisition development during the prior program, full mapping of the mean and rms velocity (two components) and temperature fields was accomplished through point measurements by LDV and Raman spectroscopy. These measurements have been documented in Refs. A and B in the REFERENCES AND PUBLICATIONS section of this report. Since this was a one year program, most of the publications are listed as "to be published". Reference B is appended to this report. A major finding of the program is that in this flow the nitrogen concentration (from the Raman measurements) is an excellent measure of the temperature. This occurs because of the preponderance of nitrogen in the flow and relatively low bleed rates of combustibles.

Considerable effort was then expended in an attempt to gain the turbulent heat transfer in a direction perpendicular to the tunnel axis. This is the dominant direction of heat transfer and it was to have been compared with the analytical modeling. The measurement involves simultaneous measurement of temperature (by Raman) and the vertical component of velocity (by LDV). After development of data acquisition software and development of measurement technique, serious multiple breakdowns of the linear flashlamp pumped dye laser occurred. Time lost in repair prevented the desired measurements from being made.

Analytical Effort

a. Analytical Modeling

At the beginning of the program year a difficulty in the then existing two equation turbulence model prevented reattachment (one important feature of the flow) from being unambiguously defined. This was traced to treatment of flow near the wall which suffered a lot of numerical noise in the region near reattachment. This was corrected by grid refinement and curve fitting of the velocity near the wall. The primary results are that a) the lengthening of the reattachment zone upon combustion is adequately predicted but b) this analysis method predicts too short a reattachment length as compared with experiment. This is accepted as a limitation of the two equation turbulence model used in this program. Another problem is that the "flame" zone is predicted to lie too close to the wall. Centrifugal force effects are known to be poorly treated by this model in the form used, and this is the place to look in future efforts.

b. Fractal Geometry

The majority of results in this program were attained by the development of fractal geometry and its application to several areas. The student assigned in this area needed some introduction to the subject and first tackled the application of fractal geometry to burn rate prediction of composite propellants. While not under the purview of this program, this work is reported as Ref. C, because it was a useful training exercise for actual work on the program.

Two areas were then pursued. First, the co-PI's original development of fractal interpolation of turbulent data traces required a very large number of data points for implementation. In this program a new method was developed for fractal dimension determination and fractal interpolation which drastically reduces the number of data points needed and, at the same time, allows interpolation of points attained at unequal time intervals. The latter eature is especially important in dealing with LDV data, for example. This work is described in Ref. D. The method was to have been applied to the joint LDV-Raman data, but, as mentioned above, the data were never attained. As a consequence, it was applied to a problem in spatial cross correlation velocimetry discussed in Ref. E.

The second area was in development of the hidden variable fractal interpolation technique, whereby two joint data traces are to be interpolated in a three dimensional space. Because of the low repetition rate of the Raman laser, the data obtained are sparse in the sense that neighboring data points are uncorrelated. The same is not true for LDV operating at high data rate. A method was developed using the LDV data as the "well known" data trace to drive the interpolation of the Raman trace to produce data points in between the actual data points. The primary assumption is that the fractal dimension for the two are, in fact, the same. This assumption has been verified, at least in this flow. Since, however, the joint data were never attained, the method could not be applied here. Instead, feasibility of the method was demonstrated using a contrived problem. The results are in Ref. D.

REFERENCES AND PUBLICATIONS

A. Wu, M.Z., Walterick, R.E., de Groot, W.A., Jagoda, J.I., and Strahle W.C., Turbulent diffusion flame properties behind a step, AIAA Paper No. 91-0079, 1991

B. Wu, M.Z., Walterick, R.E., de Groot, W.A., Jagoda, J.I., and Strahle W.C., Turbulent diffusion flame properties behind a backward facing step, J. Prop. Power (accepted for publication), 1992

C. Marvasti, M.A. and Strahle W.C., Burning rate prediction of composite solid propellants using fractal geometry, Comb. Sci. and Tech., (in press), 1991

D. Marvasti, M.A., Applications of fractal geometry in aerospace engineering, Ph.D. dissertation, Georgia Institute of Technology, 1991

E. Marvasti, M.A. and Strahle, W.C., Spatial cross correlation velocimetry using fractal geometry, submitted to 24th Symposium (International) on Combustion, 1992

OTHER INTERACTIONS AND PRESENTATIONS

A. Jagoda, J.I., Turbulent diffusion flame properties behind a step, AIAA Paper No. 91-0079, 29th AIAA Aerospace Sciences, January,1991

B. Marvasti, M.A., Fractal numerics in turbulent combustion, 4th International Conference on Numerical Combustion, December, 1991

PARTICIPANTS

Co-Principal Investigators

Dr. Warren C. Strahle

Dr. Jechiel I. Jagoda

Research Engineer

Mr. Ronald E. Walterick

Students Graduated

Dr. Mazda A. Marvasti, Ph.D., December, 1991

Mr. Michael Schuette, M.S., September, 1991

Dr. M. Z. Wu, Ph.D., (expected) January, 1992

AWARDS

No new awards.

PROGRAM MANAGER INFORMATION

Appended is the experimental work summary, Ref. B above.

TURBULENT DIFFUSION FLAME PROPERTIES BEHIND A BACKWARD FACING STEP

M.Z. Wu*, R.E. Walterick+, W.A. de Groot#, J.I. Jagoda** and W.C. Strahle++

School of Aerospace Engineering
Georgia Institute of Technology
Atlanta, GA 30332

Abstract

Experiments and analysis are reported for a subsonic combustion windtunnel experiment, in which a turbulent diffusion flame is stabilized behind a backward facing step. A mixture of hydrogen plus a diluent is introduced through the porous floor behind the step. Velocity and temperature distributions were measured using laser Doppler velocimetry and Raman spectroscopy. The flow field was modeled analytically using a two-equation turbulence model with Favre-averaged equations using the conserved scalar approach. Dominant features of the flow are a flame anchored primarily in the shear layer, a relatively cool recirculation zone and a long reattachment region compared with that for cold flow. The intensity of the Stokes line of nitrogen is shown to be an indication of the temperature of the flow. The analysis, which gave excellent agreement with experimental results in the absence of combustion, under-predicts the extent of the recirculation zone and places the region of highest temperature closer to the floor than was observed experimentally, once a flame is present.

++ Regents Professor, Fellow AIAA
** Associate Professor, Member AIAA
# Research Engineer, presently at Sverdrup/NASA LRC, Member AIAA
+ Research Engineer
* Graduate Research Assistant, Student Member AIAA

Nomenclature

c concentration
H stepheight
T temperature
U axial velocity
V vertical velocity
X axial distance
Y distance above the tunnel floor

Subscripts

rms root mean square
inf indicates axial velocity at the step

Introduction

All practical combustors require a flame anchoring region near the head of the combustion chamber. In this region the flow must be highly turbulent in order to facilitate mixing of the fuel with the oxidizer while containing areas in which the mean flow velocity is sufficiently slow that the fuel may be burned. In the case of a solid-fueled ramjet (SFRJ) the flame is normally held by allowing the air required for combustion to flow over a backward facing step[1]. Such a flow exhibits a very turbulent shear layer and low flow velocities in the recirculation region behind the step. It is the purpose of this study to investigate the complex, turbulent, reacting flow field which is generated when a fuel is injected into the recirculation zone resulting from a flow of air over a backward facing step.

In this study, the solid fuel is simulated by injecting a mixture of hydrogen and a diluent through a porous plate behind the step. This results in a "clean" flame which can be probed using modern optical techniques. The velocity field was measured using two-component laser Doppler velocimetry (LDV) while the distribution of nitrogen was determined using Raman spectroscopy. The Raman results were also used to estimate the temperature distribution throughout the flow field. A modified k-ε model with fast reaction kinetics had been developed and was used to predict the properties of the flow. The calculated results are then compared with the data obtained from the measurements.

Earlier, measurements and predictions were carried out for the cold (i.e., non-reacting) flow case. In that investigation the fuel flow was replaced by a bleed flow of carbon dioxide. The flow field was mapped using LDV measurements and local mixing was determined by Rayleigh scattering. The code was run without chemical reaction to predict the flow field. Agreement between the results of the experiments and the calculations was found to be excellent[2-4].

Various other researchers have investigated non-reacting[5,6] or reacting[7] flows over backward facing steps. However, in the reacting flow study[7] fuel and air were premixed before they entered the test section over the step. To date, the work reported here represents the only study of a reacting flow over a step in which the fuel is injected through a porous floor behind the step, resulting in a non-premixed flame clean enough for optical diagnostics.

Experimental Work

The facility used in this investigation is shown in Fig. 1. It has been described in detail elsewhere[8]. Briefly, air is drawn from the laboratory through a bellmouth shaped inlet and a boundary layer development section over a backward facing step into the test section. The floor of the tunnel behind the step consists of a porous steel plate through which gaseous fuel, which simulates the pyrolysis products of the solid fuel, is bled into the recirculation zone. The flow is then passed through a diffuser into a settling chamber before it enters a blower which discharges the combustion products to the outside. The test section is 42 cm wide, 10.5 cm high and 42 cm long. The step which stretches over the entire width of the tunnel is 3.5 cm high. In order to limit the amount of hydrogen used and to prevent overheating of the porous plate, the porous floor is divided into three sections. The first 7 cm are blocked off. A mixture of hydrogen and a diluent is injected through the next 14 cm, while inert argon or nitrogen is bled through the final 21 cm of the porous tunnel floor. The walls of the test section are made of optical quality quartz to permit optical access. The roof of the tunnel contains access ports for introducing probes such as thermocouples.

Velocity measurements were carried out using a TSI laser Doppler velocimeter equipped with Bragg cells in order to be able to detect the reverse flow in the recirculation region. The data were processed by counters and reduced using an HP A700 computer. The measuring volume of the velocimeter is an ellipsoid whose semi-major and semi-minor axes are 0.25mm and 0.035mm, respectively. The semi-major axis is aligned parallel to the tunnel floor and at right angle to the flow direction.

The Raman system is shown schematically in Fig. 2. It consists of a Candella Model LFDL-6 pulsed, linear flashlamp pumped dye laser using rhodamine 590 as the dye. It provides, nominally, one joule of energy per pulse for a duration of one microsecond at a repetition rate of ten Hertz. The resulting beam is focused into the test region by a 35 cm focal length lens. The scattered light is collected by a large diameter lens whose f-number is 2.4. The lens collimates the collected light which is refocused by an identical lens onto a spatial filter. A small focal length lens of identical f-number then re-collimates the beam before it is passed through a Raman notch filter. This filter eliminates much of the Rayleigh scattered light by removing only the light at the same wavelength as the incident laser beam.

After the scattered light emerges from the notch filter it is focused onto the entrance slit of a Spex Model 1870 spectrograph. This spectrograph was chosen for its large exit plane. This exit plane carries a polychromator which consists of a number of independently variable slits, each of which has a photomultiplier mounted behind it. In the present investigation the concentration of nitrogen in the flow was determined by measuring the intensity of its Stokes line. For an incident wavelength of 593nm the Raman Stokes line is located at 688nm. One of the exit slits was, therefore, placed at the corresponding location in the exit plane of the spectrograph. The photomultiplier used in this investigation was selected for its high sensitivity at long wavelengths. The output from the photomultiplier was dropped across a 10 kW resistor and passed into a Stanford Model SR 250 integrating amplifier before being entered into the computer. The LDV and Raman setups are mounted on separate tables on opposite sides of the test section. Each of the tables can be moved independently in all three directions.

The performance of the Raman system was checked by measuring the nitrogen concentration in streams of pure nitrogen and air. This check was repeated before each test, and measurements were only carried out if the ratio of the Stokes line intensities for the two streams was within 5% of 0.79. In addition, the performance of the system at elevated temperatures was tested. This was deemed necessary because the low number density of nitrogen molecules at high temperatures reduced the intensity of the Raman shifted line and, thus, decreased the signal to noise ratio. For this purpose, excess air was added to the combustion products of a lean, premixed hydrogen-air flame. This resulted in a hot flow whose mole fraction of nitrogen was very close to that of air. The nitrogen concentrations in this hot flow and in air at room temperature were then measured using Raman scattering. From the ratio of these nitrogen concentrations and the room temperature, the temperature of the diluted combustion products was calculated using the perfect gas law. When the optics was properly aligned and the monochromator slit width was widened sufficiently to include the Raman vibrational band of nitrogen, these temperatures agreed with those measured using an uncoated 0.003" diameter Pt - Pt/Rh thermocouple to within 50 K.

During preliminary Raman measurements inside the tunnel, it proved impossible to obtain a ratio of 0.79 between the Stokes line intensities determined for air and pure nitrogen flows. It was found that this was caused by small amounts of light scattered by the tunnel windows and walls. Some of this light entered the Stokes line photomultiplier, in spite of the notch filter and the rejection in the spectrograph. It, therefore, became necessary to remove this noise from the Raman signals. The level of stray light detected by the system was determined by filling the test section with argon and measuring the intensity of light received by the nitrogen Stokes line photomultiplier. Since no nitrogen was now present, any signal detected by the photomultiplier was noise. The noise levels were determined at all locations in the tunnel at which Raman measurements were carried out. Once this noise was subtracted from the measured Stokes line intensities the system performed satisfactory.

Model Description

The numerical code used in this study is a heavily modified version of the original, two-dimensional elliptical solver developed by Patankar and Spalding[9]. Its current version, which is described in detail elsewhere[10], is based upon the two-equation k-ε turbulence model and a hybridized upwind-central differencing scheme, to calculate the steady-state fluid properties in an incompressible, but variable density, flow behind a backward facing step. Favre averaging of the conservation equations is presumed to take account of the variable density effects. Allowance is made for a low speed fuel mixture to be injected transversely to the flow direction behind the step.

Because of the fast kinetics of a hydrogen-air reaction, thermodynamic equilibrium conditions are assumed to exist throughout the flow field. Species and, therefore, temperature fluctuations were neglected. It has been shown if Ref. 10 that consideration of these fluctuations would have lowered the temperature in the flame region by about 200 °K. However, the main flow structure would have remained unaltered[10]. Including these fluctuations substantially increases run times[10]. Further assuming adiabatic wall conditions and a Lewis number of unity allows the enthalpy and species continuity equations to become fully similar. Thus, a mixture fraction equation for the fuel mixture, along with an equation of state and an equilibrium look-up table, is sufficient to achieve closure of the combustion model[10]. For wall proximity effects in the k-ε equations, a low Reynolds number law of the wall model developed by Gorski[11] is incorporated. A final modification allows a diluent gas to be transversely injected to cool the floor downstream of the fuel injection section. For simplicity this diluent was assumed to be air which has a similar molecular weight as argon which was used in the experiments.

Results and Discussion

In all the tests carried out in this study, the air drawn into the tunnel attained a velocity of 65 m/s and a turbulence intensity of 2% upstream of the step. A 1:3 hydrogen to argon mixture (by mass) was bled at a rate of 3.3×10^{-3} kg/s through the central section of the porous floor into the tunnel. This corresponds to a bleed flow rate of 0.26 meters per second which is close to the 0.2 meter per second typically observed in SFRJs[1]. Argon at a rate of 4.5×10^{-2} kg/s was introduced through the downstream-most part of the floor.

Axial velocities at a series of downstream locations, 0.1 step heights above the tunnel floor with and with out combustion are shown in Fig. 3. The locations at which the velocities switch from negative to positive are assumed to correspond to the reattachment points in these two flows. Contrary to initial expectations, the recirculation zone was found to be longer in the case with combustion than without (8.8 vs. 7.3 step heights). Similar trends were predicted by the model although the actual values of the reattachment point, 7.3 and 6.1 stepheights with and without combustion, respectively, were not correctly calculated, see Fig. 3. Here the reattachment points were calculated from the reversal of the slope of the velocity vector near the tunnel floor.

Originally, the presence of combustion was expected to shorten the recirculation zone because the expansion of the hot combustion products allows the adverse pressure gradient to reverse the flow more easily. However, the injection of cold, heavy argon both downstream of the fuel bleed section of the porous plate and as a diluent in the fuel stream apparently caused the recirculation zone to be extended.

Axial and vertical mean velocities measured at a number of vertical locations for five different axial positions are shown in Fig. 4. The axial velocities at the top edge of the shear layer are close to those of the freestream. As one moves downward, these velocities decrease rapidly and become negative close to the floor since all five axial locations shown lie within the recirculation zone.

Vertical velocity profiles at the same five axial locations in the test section are also shown in Fig. 4. These data are of special interest, since vertical velocity components control the rate of convective heat transfer from the flame to the propellant. Convective as well as radiative heat transfer, in turn, control the burn rate of the solid propellant. Since all five axial locations lie in the downstream half of the recirculation zone, the vertical velocity components are generally negative, i.e. downwards. Above one stepheight over the tunnel floor the vertical velocity component is negligible. As one moves lower in the test section the downward velocity increases until it reaches a maximum at .4 stepheights above the tunnel floor. Closer to the floor the downward velocity decreases but does not turn upwards in the region accessible by LDV. This indicates that the bleed flow is unable to penetrate far into the test region before it is entrained by the recirculating flow which carries it along the floor of the tunnel towards the step and then up, towards the flame.

Figure 5 compares the measured streamlines which represent the flow field without and with combustion. Clearly, the presence of combustion extends the length of the recirculation zone. The flame also appears to accelerate the flow away from the shear layer towards the porous floor of the tunnel. The flow turns more sharply away from the flame in the shear layer in the presence of combustion. Figure 6 shows the streamlines for the corresponding section of the flow field predicted by the code without and with combustion. The code significantly under-predicts the extent of the recirculation zone for both cases. In addition, near reattachment the model predicts the shear layer to be much closer to the floor of the tunnel than measurements would indicate.

The local concentrations of nitrogen were determined at the same locations as the velocities shown in Fig. 4 by measuring the intensities of the Raman Stokes lines of nitrogen at these points. Figure 7a shows the resulting distributions of the nitrogen concentrations. The concentration of nitrogen decreases dramatically as one moves from the freestream down into the shear layer. Once the shear layer has been crossed the level of nitrogen begins to increase again slightly.

In order to determine to what extent the observed low levels of nitrogen in the shear and recirculation zones are due to the argon diluent in the bleed gas, this argon flow was replaced by an equal flow of nitrogen and the Raman measurements were repeated. If the concentration of bleed gas in the recirculation zone were to be significant, the local concentrations of nitrogen should be higher if nitrogen rather than argon was used as the diluent. The measured nitrogen concentrations using nitrogen and argon as the bleed gas diluent are compared at station X/H = 6.96 in Figure 7a. Since no difference in nitrogen concentration was observed, it may be concluded that the concentration of bleed gas in the recirculation zone is small. Instead, the bleed gas is carried by the recirculatory flow along the tunnel floor and the step towards the shear layer, where its fuel burns. A similar conclusion has also been arrived at in the discussion of the flow field, above. This suggests that the recirculation zone consists, primarily, of nitrogen. Therefore, the variation of the concentration of nitrogen shown in Fig. 7a must be predominantly an effect of temperature. Thus, an estimate of the local temperatures in the recirculation region can be obtained from the measured nitrogen concentrations using the perfect gas law. It must, however, be remembered that these temperatures can only be approximate since the presence of other species has been neglected.

Figure 7b shows the vertical temperature distributions calculated from the nitrogen concentrations in Fig. 7a. At X/H = 6.23 in Fig. 7b the results obtained with an uncoated Pt/Pt10%Rh, three micron diameter thermocouple have also been added. The mean temperatures measured by the thermocouple are quite comparable to those obtained from the Raman measurements. However, the thermocouple cannot follow the rapid fluctuations of the temperature in this highly turbulent flow.

The flame appears to be confined to the shear layer with the maximum temperature coinciding with the location at which the flame front was visually observed. The temperature is significantly lower in the recirculation zone. This indicates that no significant combustion takes place in this region and that some heat is transfered to the tunnel floor.

The temperature distribution at 4.76 stepheights behind the step calculated using the model is compared with experimental data in Fig. 7b. Clearly, the agreement is not good. Just like the shear layer (see Fig. 6), the predicted flame positions itself much closer to the tunnel floor than the measurements and visual observations would indicate for the conditions under investigation. The flame could only be raised to the experimentally observed position if the fuel flow rate was increased. It is also possible that agreement would be improved if the turbulent temperature fluctuations were included in the calculations. It thus appears that, in the absence of these temperature fluctuations, the model predicts too low a shear layer resulting in a flame too close to the floor of the tunnel. In addition, the model neglects the effect of heat transfer to the tunnel walls. If these heat losses were accounted for, the predicted density of the flow in the recirculation zone would increase. This would increase the size of the recirculation zone which would shift the reattachment point downstream and lift the flame further off the floor.

The distributions of the turbulence intensity in the test section are shown in Fig. 8. Above the shear layer the turbulence intensities both in the axial and vertical directions (Figs. 8a and 8b, respectively) are close to 5%. In the shear layer the axial and vertical turbulence intensities rises to about 18% and 13%, respectively. Both are only slightly lower in the recirculation region. Near the tunnel floor the turbulence intensities appear to increase slightly. This may be due, in part, to the increased noise in the LDV data due to light scattered by the tunnel floor. It may, however, also reflect a true increase in turbulence caused by the entry of the bleed gas. Finally, the axial turbulence intensity distribution in the cold flow has been added to the plot corresponding to X/H = 5.49. The presence of the flame appears to lower the intensity of turbulence, although no explanation can be offered for this observation at this time.

The distribution of the RMS values of the temperatures are shown in Fig. 9. The largest temperature fluctuations were observed in the region of greatest temperature gradient where the cold freestream mixes with the top of the hot shear layer.

Conclusions

1. For the conditions investigated, the combustion of the fuel injected through the porous floor behind a backward facing step takes place as a diffusion flame which is largely confined to the shear layer between the outer flow and the recirculation zone. Little combustion appears to take place in the recirculation zone.
2. With combustion, and somewhat contrary to expectations, the reattachment length increases as compared to the cold flow case. This appears to be caused by the heavy, inert diluent which was used as an injectant.
3. As opposed to the excellent agreement the cold flow, the k-ε model without turbulent temperature fluctuations does not satisfactorily predict

the hot flow. The model shortens the recirculation region and lowers the shear layer. Therefore, the flame is lowered too close to the surface.

4. The intensity of the Raman Stokes line of nitrogen is a good indication of the temperature in this system, because of the preponderance of nitrogen everywhere in the flow, except very close to the injection plate.

5. A novel method of data reduction for Raman measurements was developed, which removes the noise caused by stray light in highly reflective systems like the one investigated here.

Acknowledgement

This work was supported by the Air Force Office of Scientific Research under contract # AFOSR-88-0001. Contributions to this program by Dr. Susuma Noda are gratefully acknowledged.

References

[1] Mady, C. J., Hickey, P. J. and Netzer, D. W., "Combustion Behavior of Solid Fuel Ramjets," *Journal of Spacecraft and Rockets*, Vol. 15, May/June 1987, pp. 131-132.

[2] Richardson, J., de Groot, W. A., Jagoda, J. I., Walterick, R. E., Hubbartt, J. E. and Strahle, W. C., "Solid Fuel Ramjet Simulator Results: Experiments and Analysis in Cold Flow," *Journal of Propulsion and Power*, Vol. 1, 1985, pp. 488-493.

[3] De Groot, W. A., Latham, R., Jagoda, J. I. and Strahle, W. C., "Rayleigh Measurements of Species Concentration in a Complex Turbulent Flow," *AIAA Journal*, Vol. 25, 1987, pp. 1142-1144.

[4] De Groot, W. A., Walterick, R. E., Jagoda, J. I., "Combined LDV and Rayleigh Measurements in a Complex Turbulent Mixing Flow," *AIAA Journal*, Vol. 27, 1989, pp. 108-110 .

[5] Driver, D.M., Seegmiller, H.L. and Marvin, J., "Unsteady Behavior of a Reattaching Shear Layer," AIAA Paper 83-1712, 1983.

[6] Eaton, J.K. and Johnston, J.P., "Low Frequency Unsteadiness of a Reattaching Turbulent Shear Layer", *Turbulent Shear Flow 3*,"Springer - Verlag, Berlin, 1982, pp. 162 - 170.

[7]Pitz R.W. and Daily, J.W., "Combustion in a Turbulent Mixing Layer Formed at a Rearward Facing Step," *AIAA Journal*, Vol. 21, November 1983, pp. 1565 - 1570.

[8]Walterick, R. E., de Groot, W. A., Jagoda, J. I. and Strahle, W. C., "Combustion Test Facility and Optical Instrumentation for Complex Turbulent Reacting Flow," AIAA Paper 88-0052, 1988.

[9]Patankar, S. V. and Spalding, D. B., *Heat and Mass Transfer in Boundary Layers*, 2nd Ed., Intertext Book Co., London, 1970.

[10]Tsau, F.H. and Strahle, W.C., "Prediction of Turbulent Combustion Flowfield Behind a Backward Facing Step," *Journal of Propulsion and Power*, Vol. 6, May/June 1090, pp. 227-237.

[11]Gorski, J. J., "A New Near-Wall Formulation for the k-ε Equations of Turbulence," AIAA Paper 86-0147, 1986.

FIGURE LEGENDS

Fig. 1 Schematic of the windtunnel.

Fig. 2 Schematic of the velocimeter and Raman spectroscopy system.

Fig. 3 Distribution of axial velocities showing reattachment with and without combustion.

Fig. 4 Axial (a), and vertical (b) velocities, normalized with respect to axial velocity at the step, as a function of vertical distance, in step heights, at various axial locations.

Fig. 5 Comparison of measured flow fields without (above) and with (below) combustion as represented by their stream lines.

Fig. 6 Comparison of computed flow fields without (above) and with (below) combustion as represented by their stream lines.

Fig. 7 (a) Nitrogen concentration distributions with argon or nitrogen (dotted line) diluent; (b) Resultant temperature distributions with thermocouple (X/H = 6.23) and predicted (X/H = 4.76) temperatures shown as dotted lines.

Fig. 8 Turbulence intensity of the axial (a), and vertical (b) velocities. Axial turbulence intensity for cold flow at X/H = 5.49 (dotted line) shown for comparison.

Fig. 9 Turbulence intensity of the temperature.

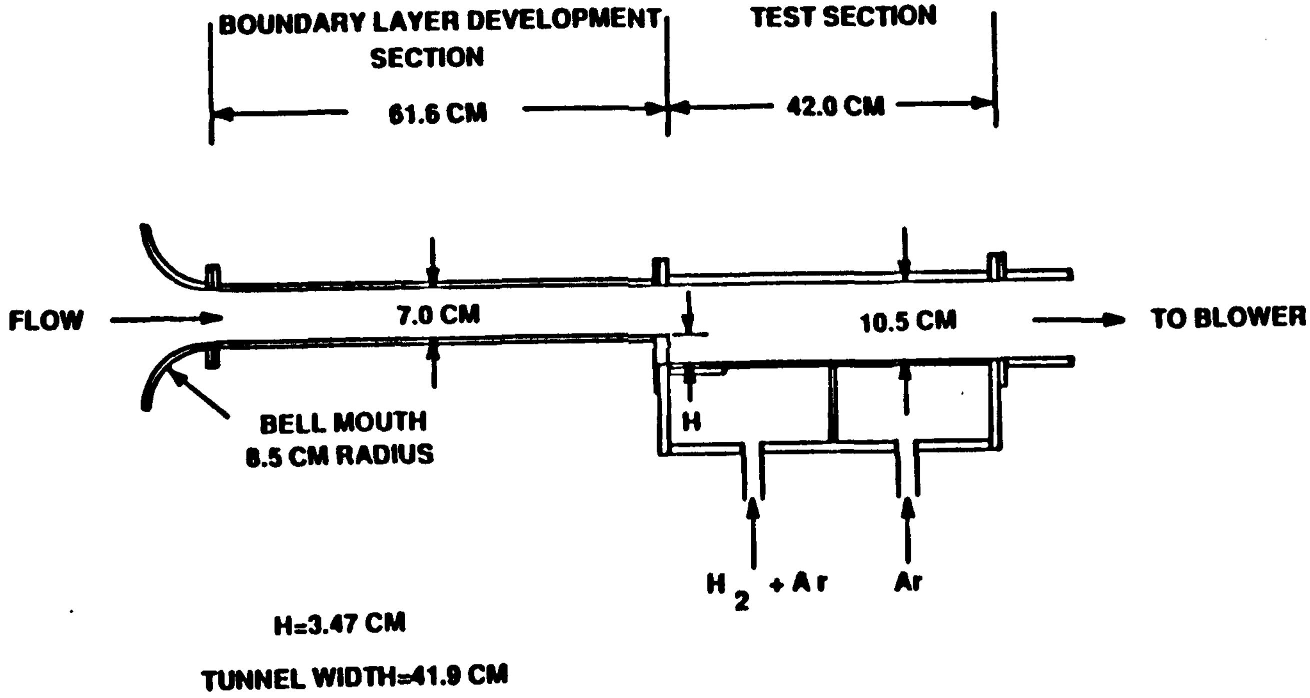

BOUNDARY LAYER DEVELOPMENT SECTION
TEST SECTION
61.6 CM
42.0 CM
FLOW
7.0 CM
10.5 CM
TO BLOWER
BELL MOUTH
8.5 CM RADIUS
H
H 2 + Ar
Ar
H=3.47 CM
TUNNEL WIDTH=41.9 CM

Fig 1

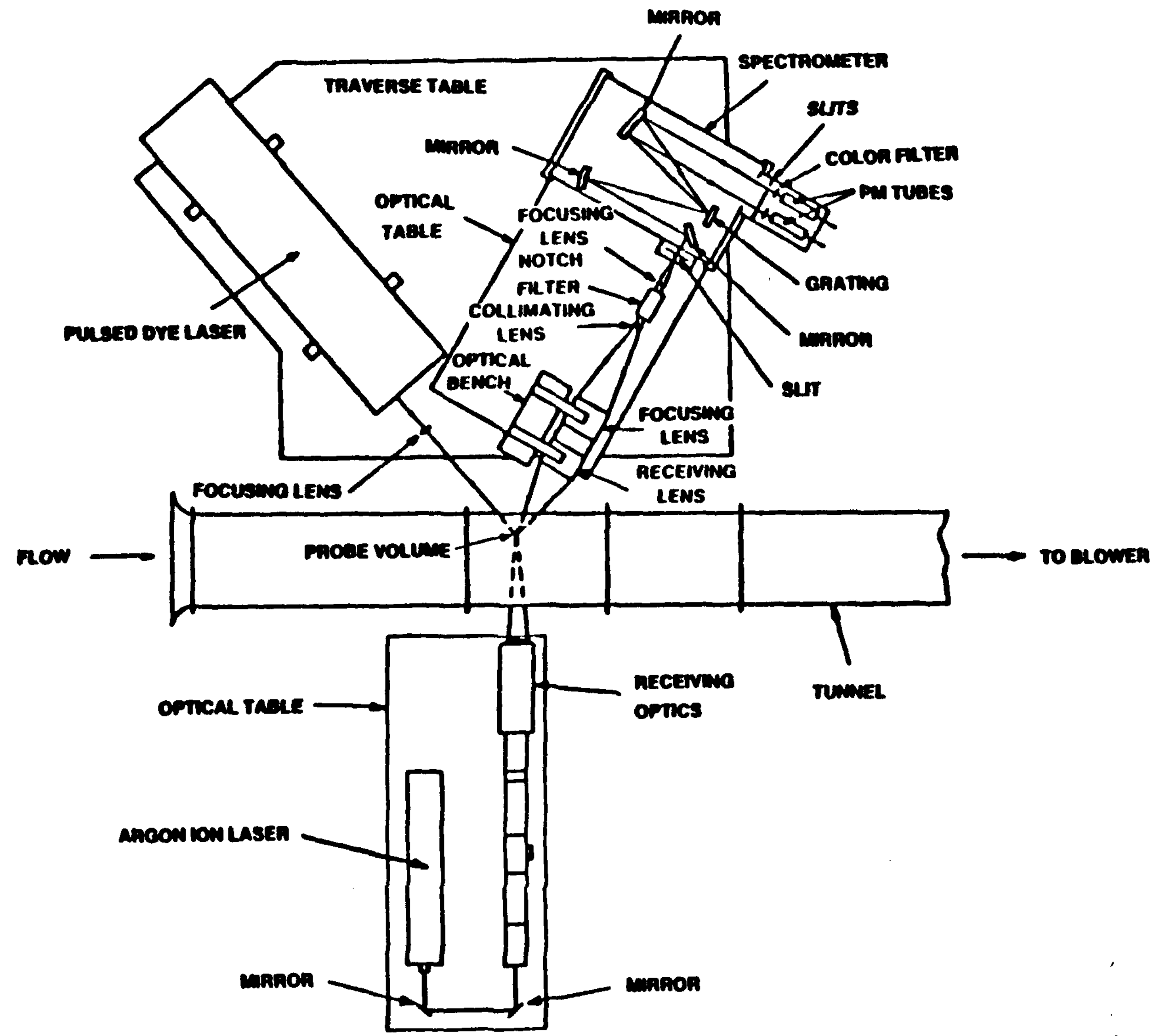
MIRROR
SPECTROMETER
TRAVERSE TABLE
SLITS
MIRROR
COLOR FILTER
PM TUBES
OPTICAL
TABLE
FOCUSING
LENS
NOTCH
FILTER
GRATING
COLLIMATING
LENS
MIRROR
PULSED DYE LASER
OPTICAL
BENCH
SLIT
FOCUSING
LENS
RECEIVING
LENS
FOCUSING LENS
FLOW
PROBE VOLUME
TO BLOWER
RECEIVING
OPTICS
TUNNEL
OPTICAL TABLE
ARGON ION LASER
MIRROR
MIRROR

Fig 2

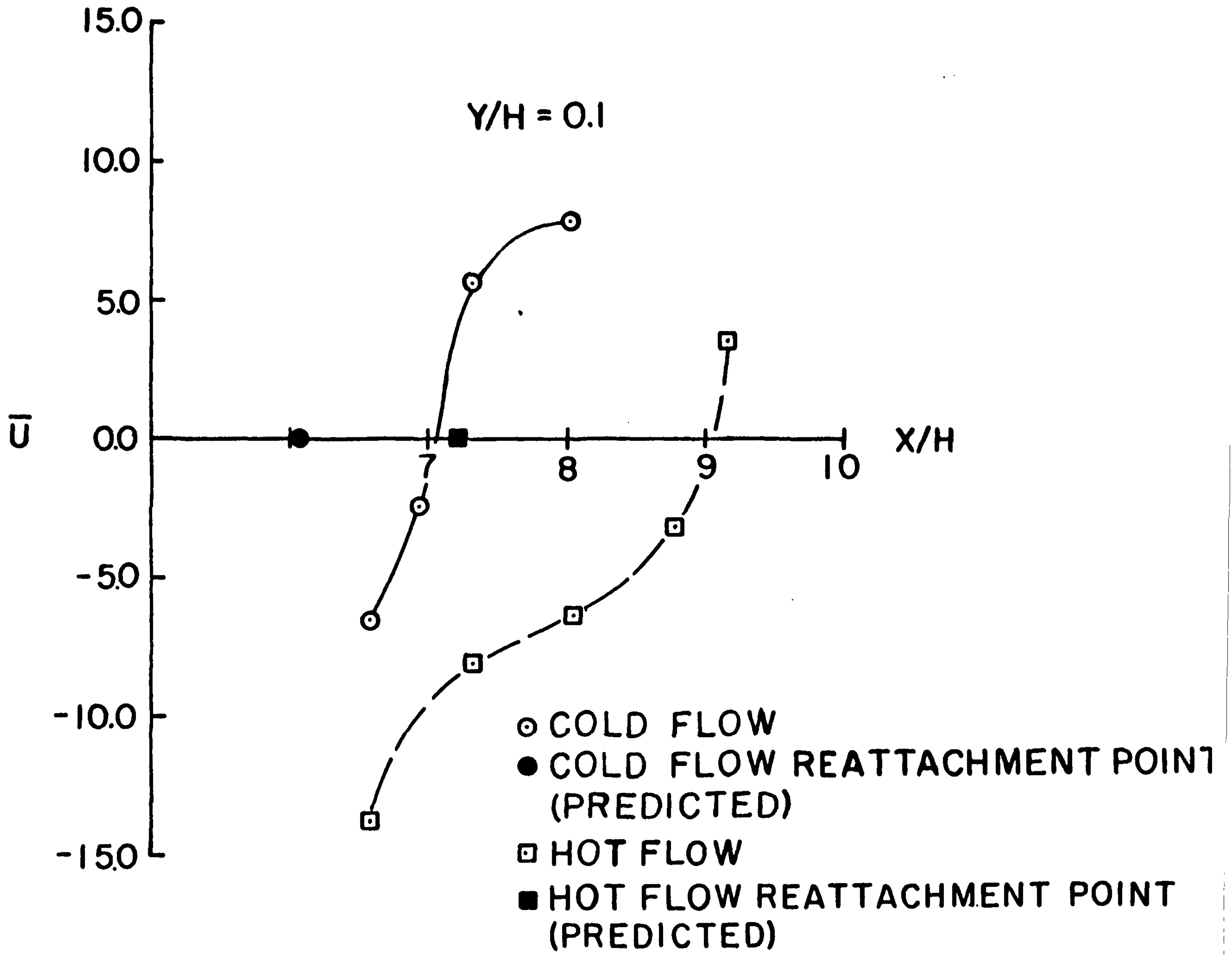
Y/H = 0.1
15.0
10.0
5.0
0.0
-5.0
-10.0
-15.0
Ū
7
8
9
10
X/H
COLD FLOW
COLD FLOW REATTACHMENT POINT
(PREDICTED)
HOT FLOW
HOT FLOW REATTACHMENT POINT
(PREDICTED)

Fig. 3

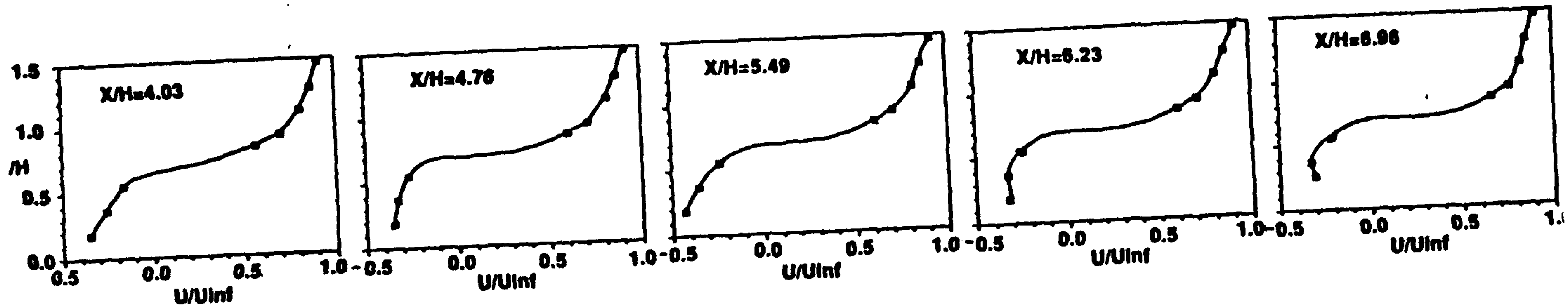
X/H=4.03
X/H=4.76
X/H=5.49
X/H=6.23
X/H=6.96
/H
U/Uinf
1.5
1.0
0.5
0.0
-0.5
0.0
0.5
1.0

a

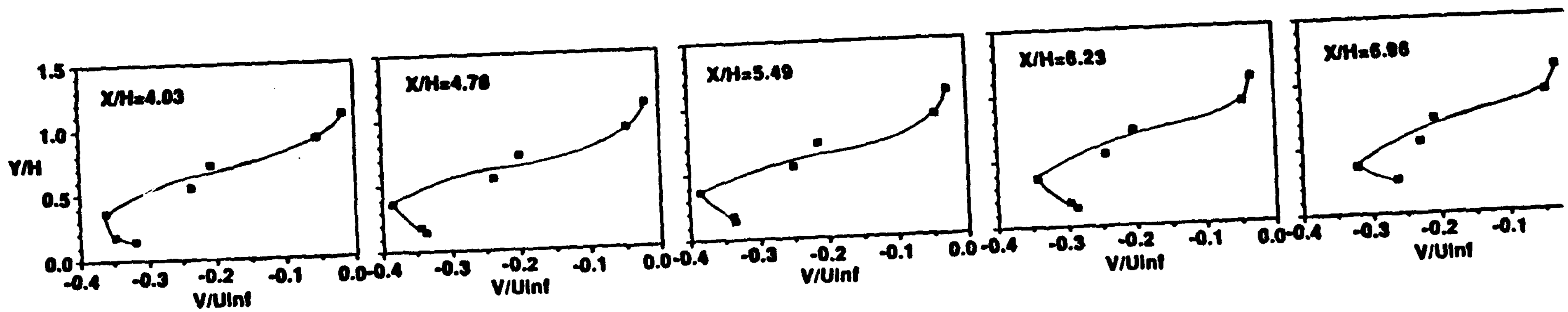
X/H=4.03
X/H=4.76
X/H=5.49
X/H=6.23
X/H=6.96
Y/H
V/Uinf
1.5
1.0
0.5
0.0
-0.4
-0.3
-0.2
-0.1
0.0

b

Fis 4

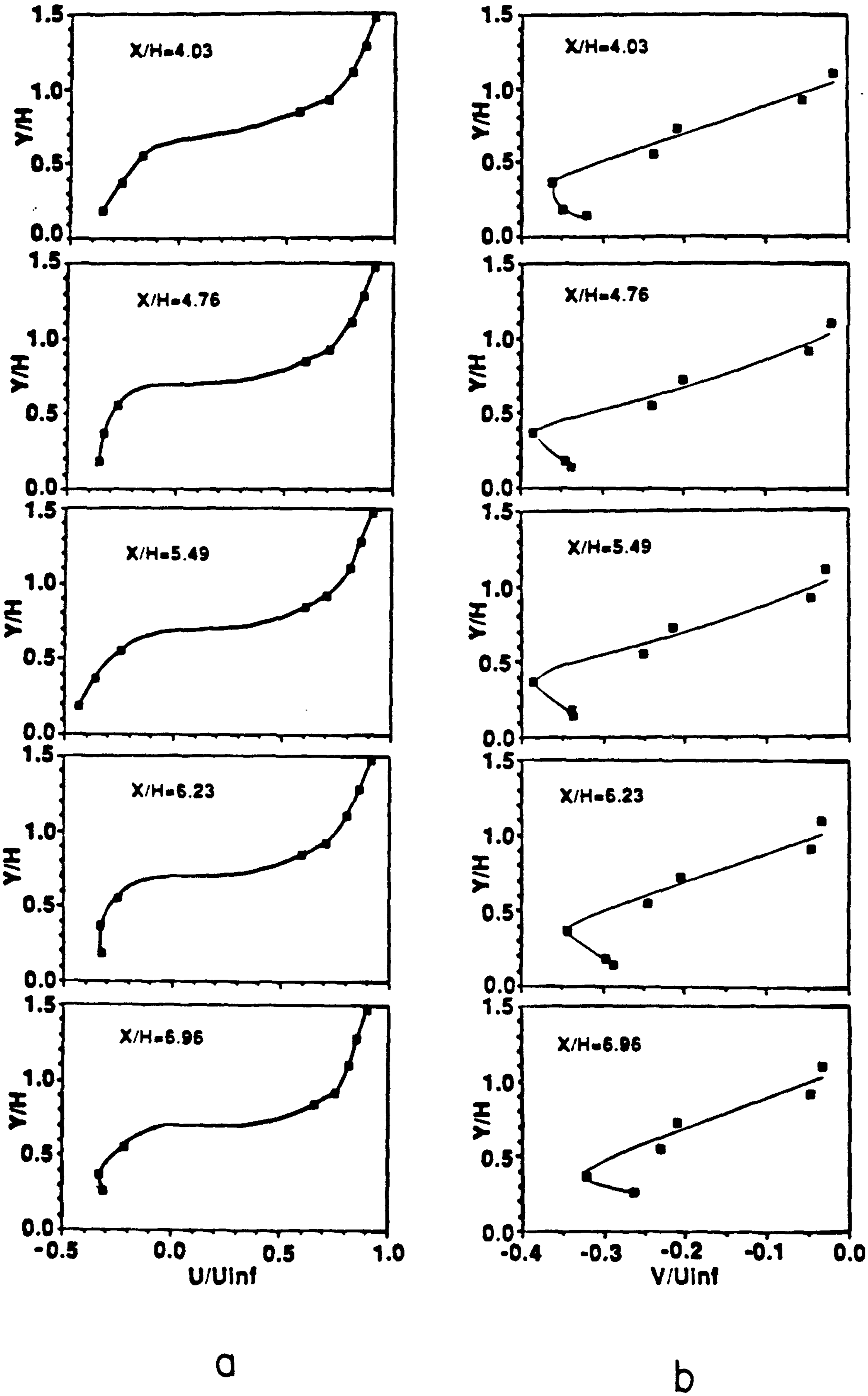

Fig 4 / al-tin

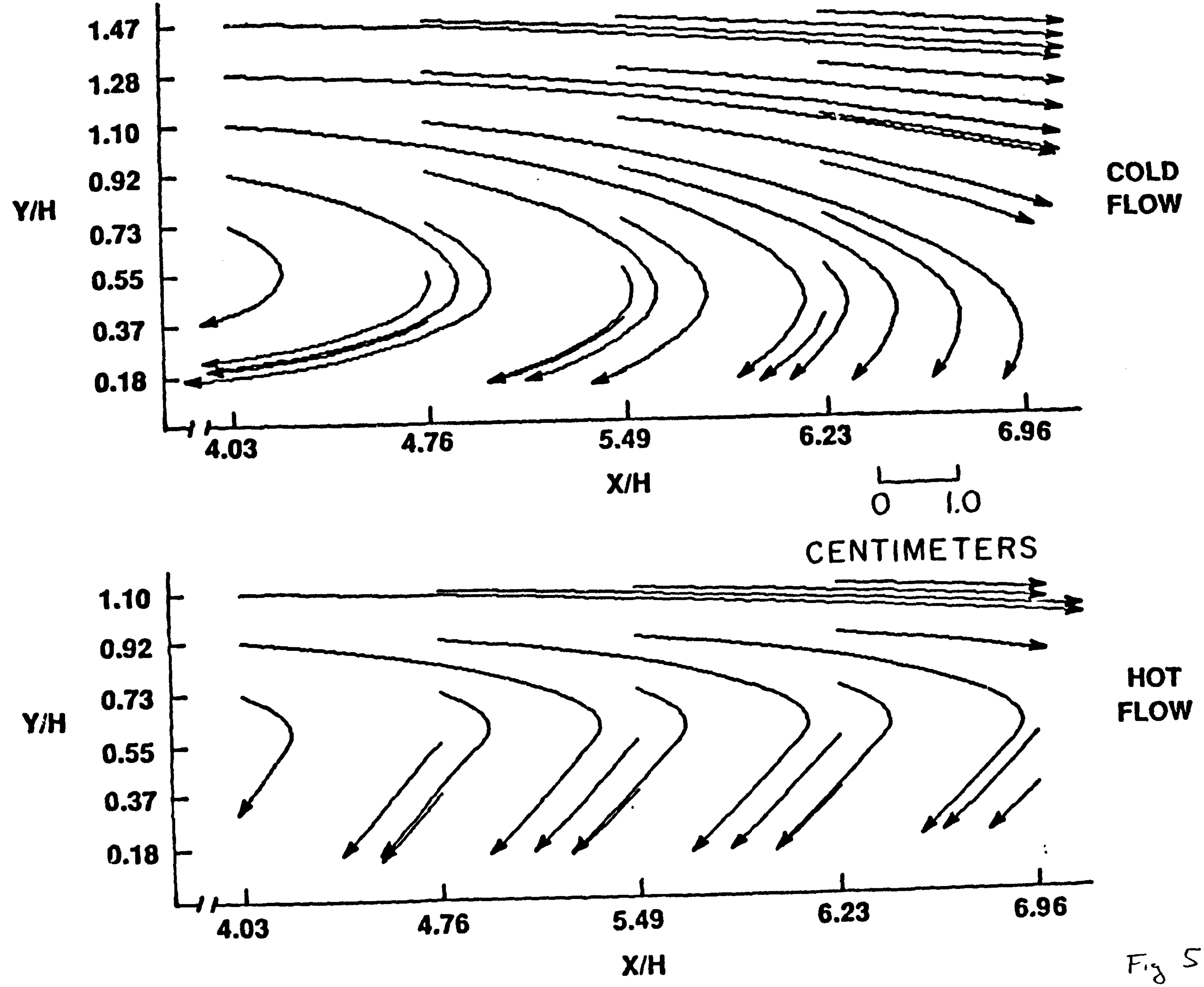
1.47
1.28
1.10
0.92
0.73
0.55
0.37
0.18
Y/H
4.03
4.76
5.49
6.23
6.96
X/H
COLD
FLOW
0
1.0
CENTIMETERS
1.10
0.92
0.73
0.55
0.37
0.18
Y/H
4.03
4.76
5.49
6.23
6.96
X/H
HOT
FLOW

Fig 5

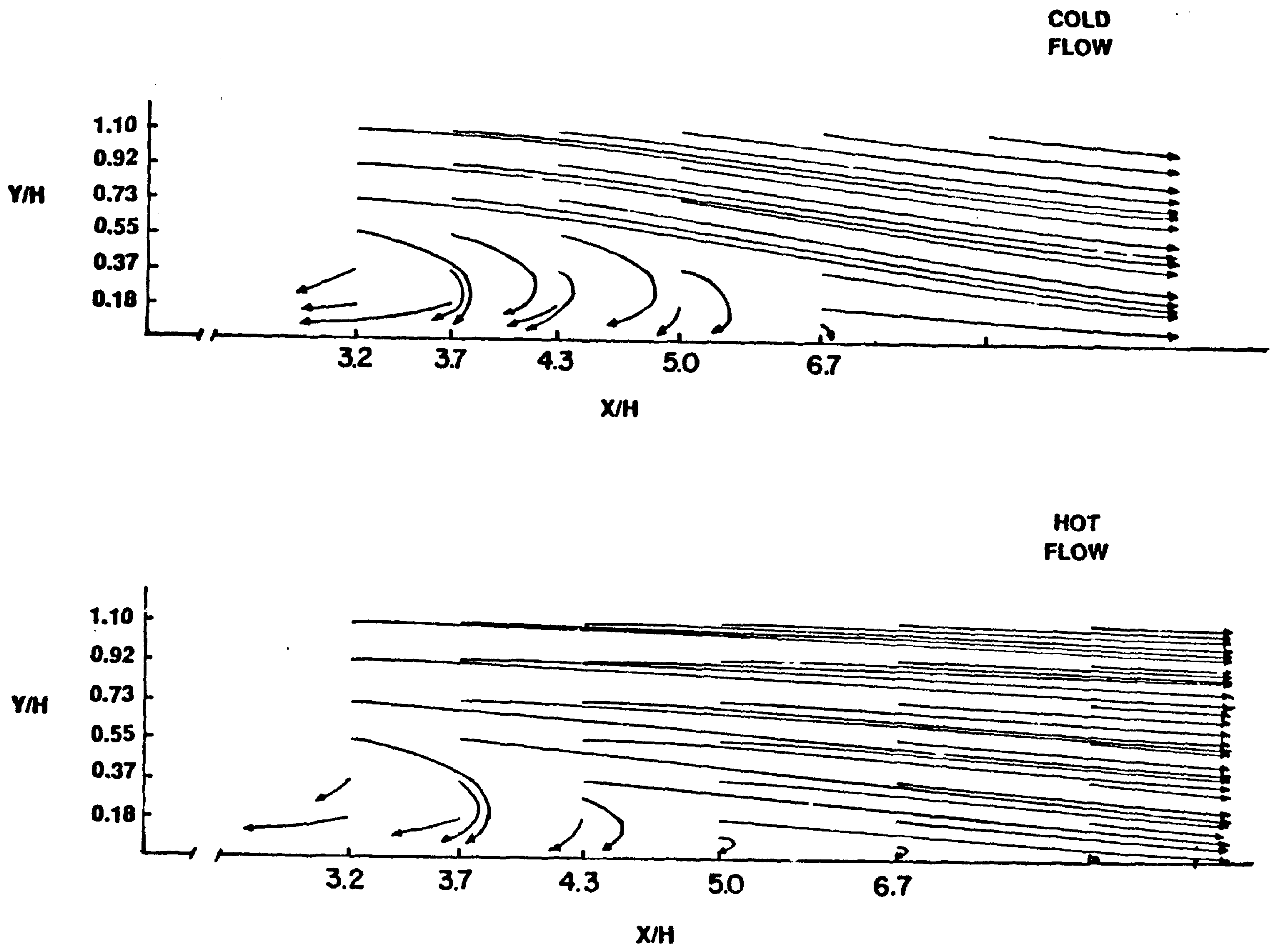
COLD
FLOW
Y/H
1.10
0.92
0.73
0.55
0.37
0.18
3.2
3.7
4.3
5.0
6.7
X/H
HOT
FLOW
Y/H
1.10
0.92
0.73
0.55
0.37
0.18
3.2
3.7
4.3
5.0
6.7
X/H

Fig. 6

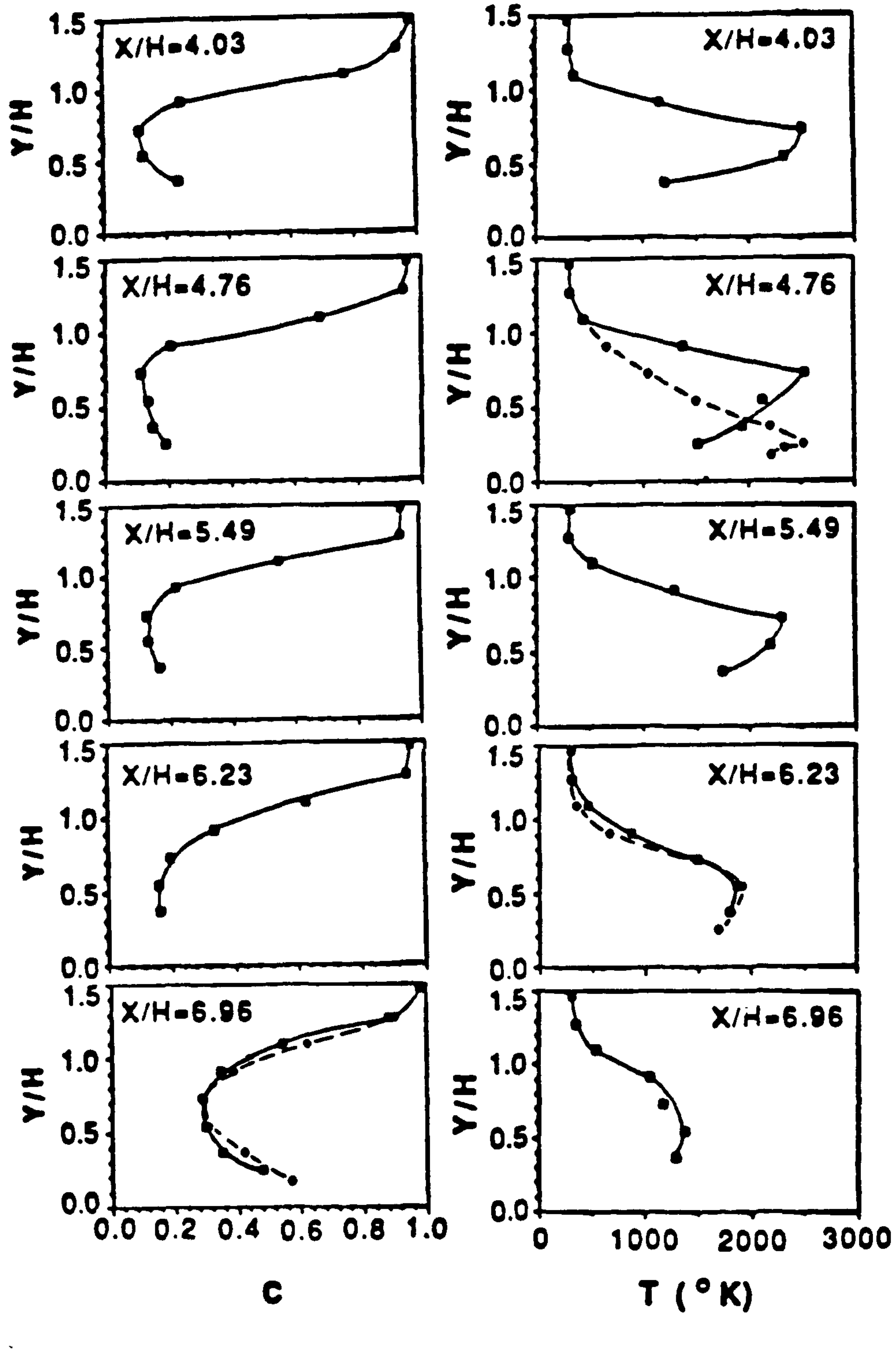

a

b

Fig 7 /aitken

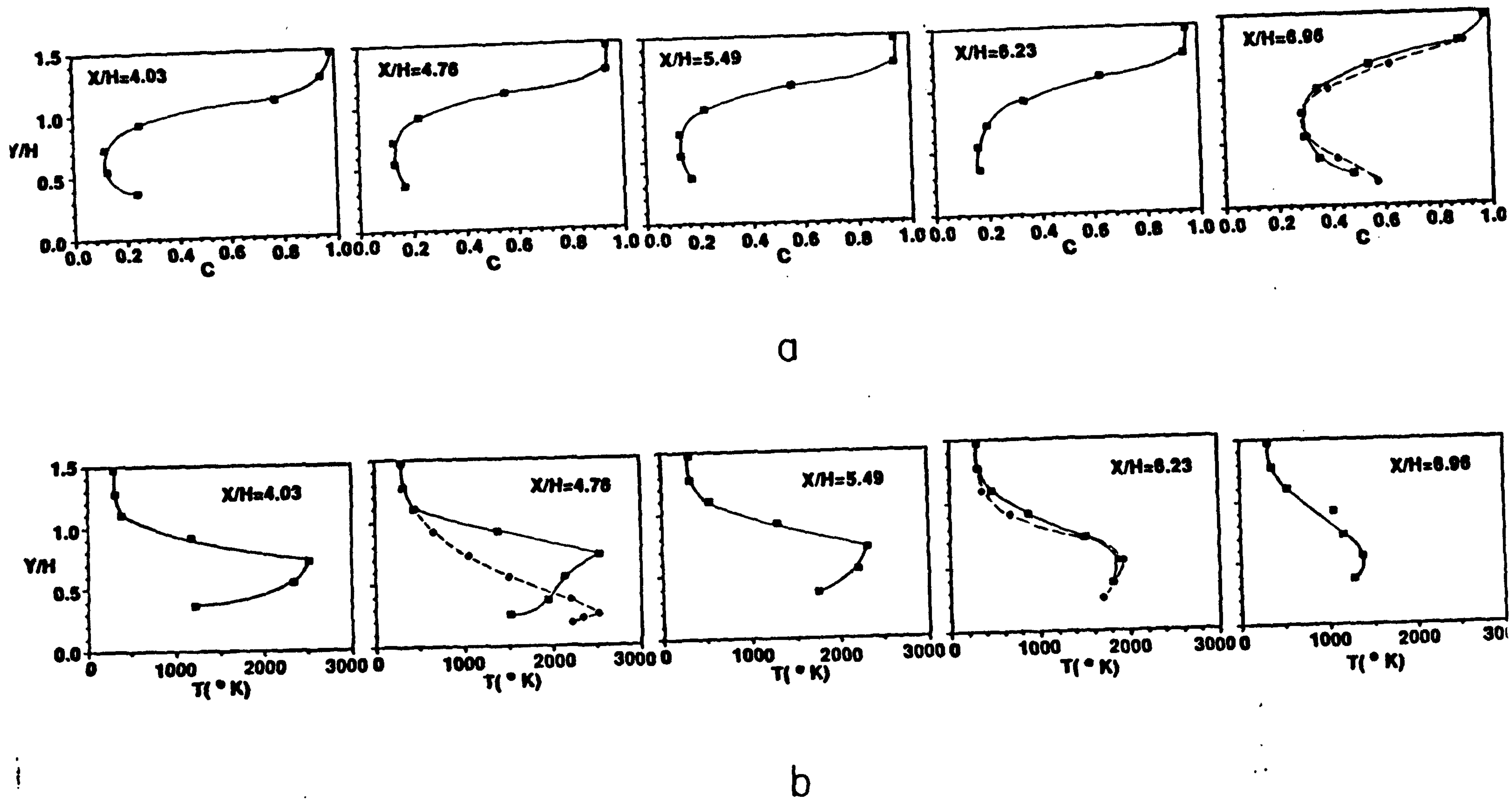

Fig 7

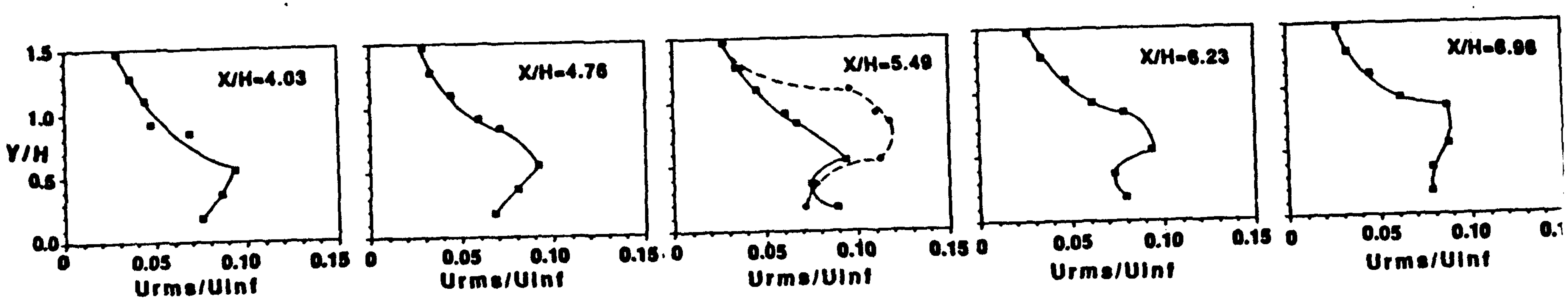
X/H=4.03
X/H=4.76
X/H=5.49
X/H=6.23
X/H=6.96
Y/H
Urms/Uinf

a

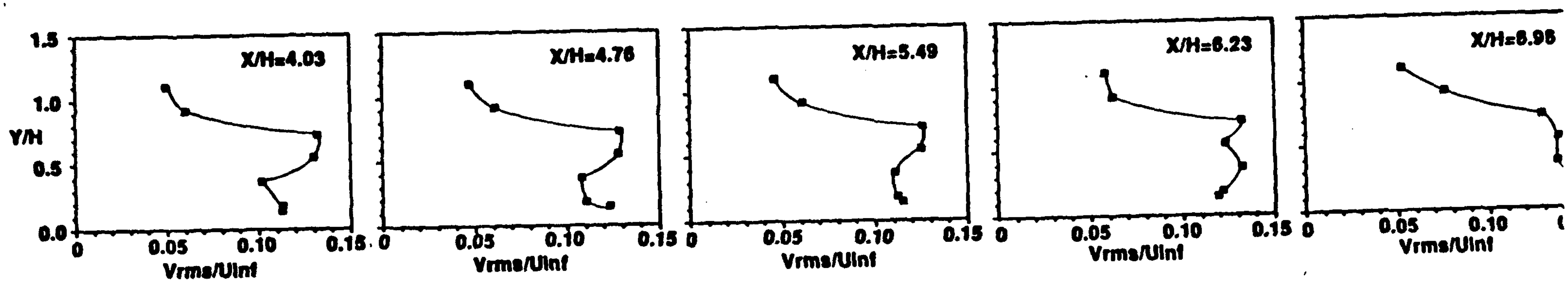
X/H=4.03
X/H=4.76
X/H=5.49
X/H=6.23
X/H=6.96
Y/H
Vrms/Uinf

b

Fig 8

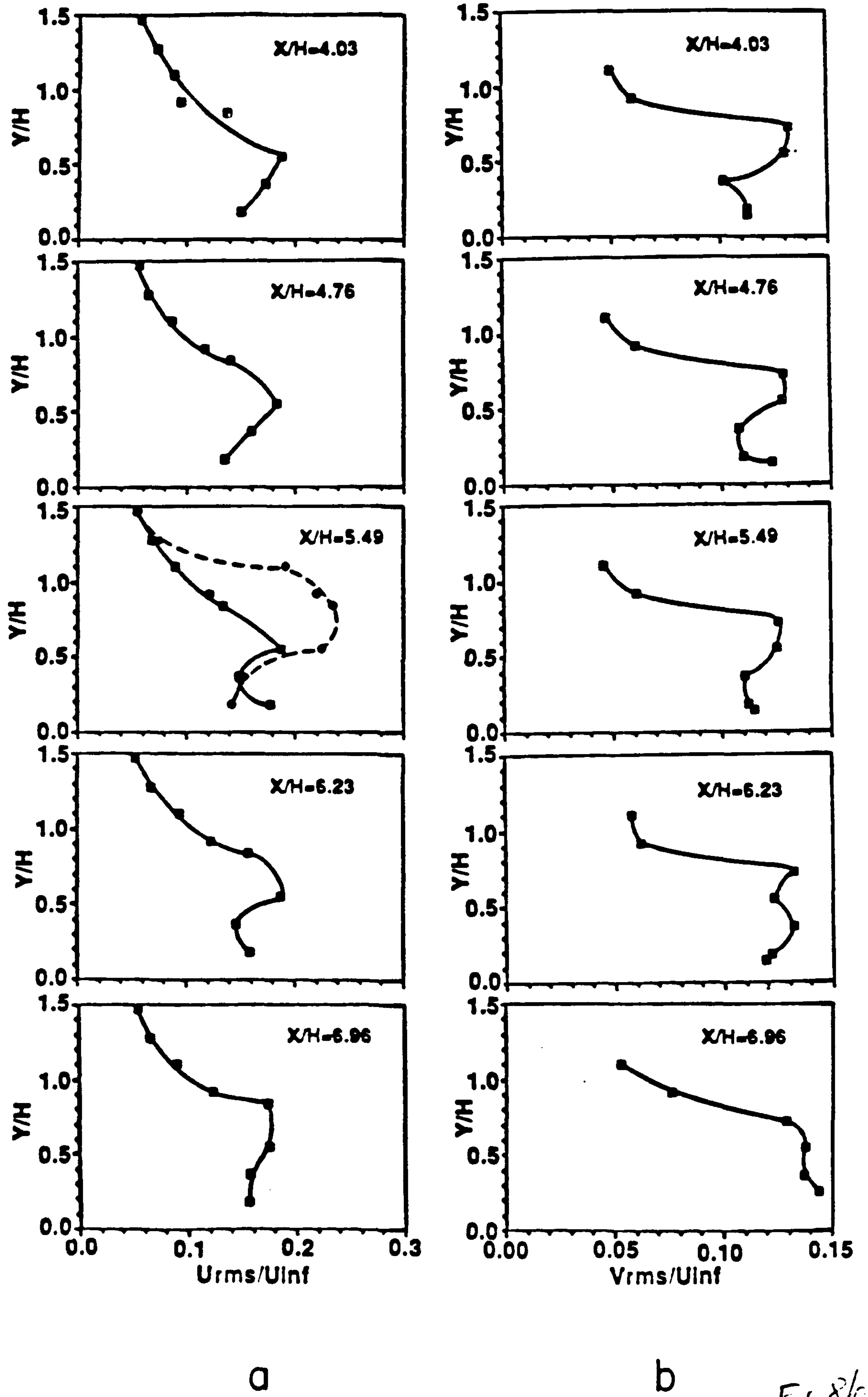

Fig 8/a...

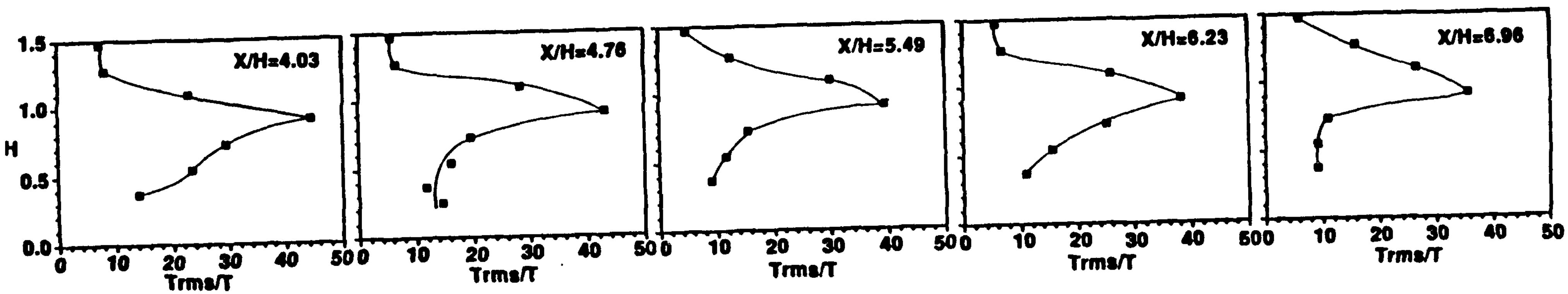
X/H=4.03
X/H=4.76
X/H=5.49
X/H=6.23
X/H=6.96
H
1.5
1.0
0.5
0.0
0
10
20
30
40
50
Trms/T

Fig 9

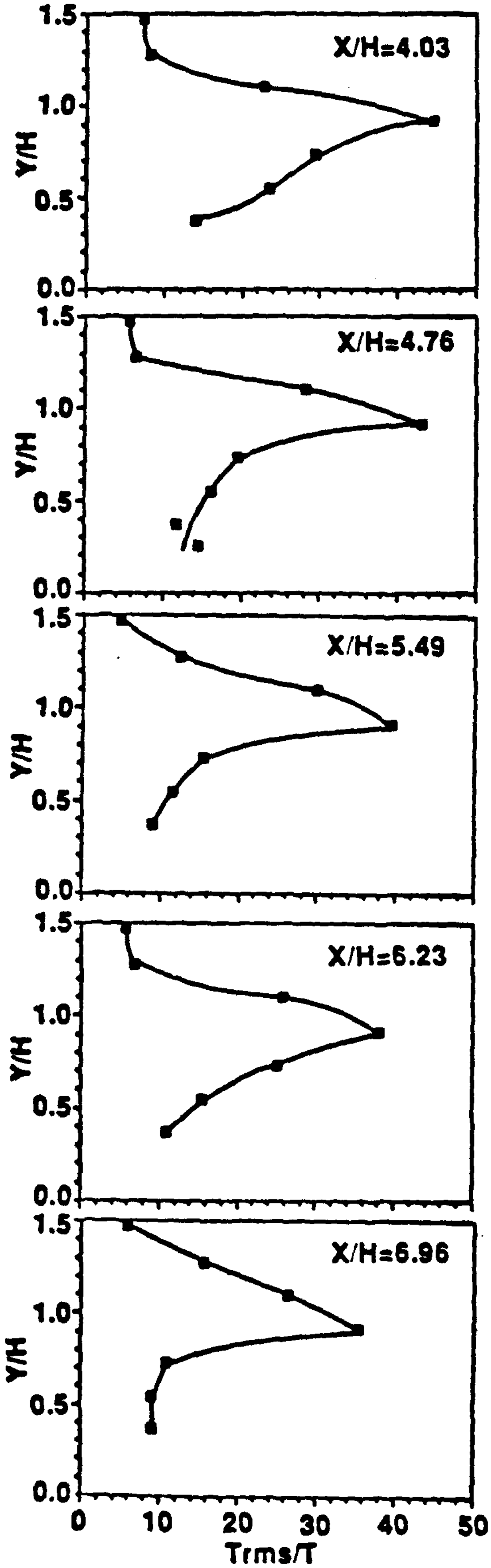
X/H=4.03
X/H=4.76
X/H=5.49
X/H=6.23
X/H=6.96
Y/H
Trms/T
0.0
0.5
1.0
1.5
0
10
20
30
40
50

Fi. 9/altern